# Robust Broadband Beamformer design for Noise Reduction and Dereverberation

**Lara Nahma · Hai Huyen Dam · Cedric Ka Fai Yiu · Sven Nordholm**

**Abstract** In this paper, we investigate robust design methods for broadband beamformers in reverberant environments. In the design formulation room reverberation as well as robustness to amplitude and phase mismatches in the microphones have been included. Particularly, the direct path and the reflections are separated in the design such that there is a penalty on the reflective part. This approach is different from the commonly studied problem of dereverberation of a single point source as the investigated design is made over a region in space. A single point derverberation is not a very practical approach due to a high sensitivity to position changes. Thus in order to obtain more practical microphone array designs, we study methods that optimize performance over areas in space. The design problem has been formulated in four different ways; (i) using direct path only representing a traditional beamformer design method, (ii) using a robust design method which considers robustness against the microphone characteristics (gain and phase) by optimizing the mean performance, (iii) by including room impulse response in the design and finally, (iv) using both robustness and room impulse response in the design. Simulation results show that robust direct path based beamformer can achieve approximately the same performance as including room response in the design in many reverberation environments. The proposed method provides robustness over larger variations in the reverberation environment. This means that the robust direct path based method which is based on mean variations in gain

Lara Nahma, Hai Huyen Dam and Sven Nordholm
Department of Electrical Engineering, Computing and Mathematical Sciences
Curtin University
E-mail:     l.alibreesm@postgrad.curtin.edu.au          S.Nordholm@curtin.edu.au
H.Dam@curtin.edu.au

Cedric Ka Fai Yiu
Department of Applied Mathematics
The Hong Kong Polytechnic University
E-mail: cedric.yiu@polyu.edu.hk

and phase can be used in low- to medium ($T_{60} = 100 - 300$ms) reverberant environments with good result.

Keywords: Near field beamformer design, de-reverberation, robust broadband beamformer, signal enhancement.

## 1 Introduction

Beamforming is a temporal and spatial processor used in conjunction with the microphone array to perform the spatial filtering. The fundamental concept of the beamforming relies on the spatial and spectrotemporal discrimination of the desired components in the presence of background noise, reverberation and interfering signals. That means the main task of the beamformer is to extract the signal that originated from the region of interest while attenuating all other signals coming from different locations [7,19,22].

Beamforming has been applied in wide variety of application fields such as communication, radar, sonar, and biomedical. The design of beamformers can be divided into two types: data independent and data dependent beamformers [26]. In the data dependent beamformer (known as adaptive beamformer) such as the generalized sidelobe canceller [21] and linearly constrained minimum variance (LCMV) beamformer [10], the filter coefficients are chosen based on the statistics of the received data to optimize the beamformer output [1,32]. For the fixed beamformer case, in contrast to the adaptive beamformers, their filter coefficients do not depend on the target source or environment conditions and are chosen based on a pre-specified beam-pattern [28,25] such as, superdirective microphone array [17] and frequency invariant beamforming [31]. The main advantages of fixed beamformers are their ability to avoid signal distortion with no requirement of control algorithms and relatively simple numerical complexity with easy implementation [4].

Generally, the broadband beamformer design problem is to calculate the filter coefficients such that the actual response of the beamformer optimally fits the desired response, which is specified depending on the target application. In the literature, there are wide variety of optimization techniques dedicated to the design of broadband beamformers such as Least Square (LS), Weighted Least Squares (WLS) [5],[24] and Minimax [23], [28] criteria.

In open space applications where the sound propagates unencumbered a free field, Green function describes the transmission between a sound source and each microphone [14]. In contrast to this scenario, we have indoor applications, where the sound wave propagates inside an enclosure. In this situation, the microphone signals contain not only the direct path source signal but also delayed and attenuated duplicate signals created by reflections from the enclosure and objects inside it. For this scenario, the room impulse response (RIR) becomes more complex [6,11,16,22].

Joint dereverberation and noise reduction algorithms have become a major research subject in the last decade since reverberation and noise typically result in a degradation of speech quality and intelligibility as well as reduced listen-

ing comfort. Recently renewed interest in such algorithms have been driven by commercial speech recognition applications. Many different studies have been done in reverberant environments while considering different aspects of processing [19]. In the paper by Li et. al. [16] several multi-criteria optimization models was formulated based on L-1 norm for the fixed indoor beamformer design. The proposed method separates the early and late reverberation in the design process. A two stage beamforming approach was proposed for dereverberation and noise reduction [11]. A combination of fixed and adaptive beamformers has been employed in two stage approach to achieve a joint dereverberation and noise reduction. In [3] a combination of MVDR beamformer and signal channel spectral enhancement scheme was presented for a joint dereverberation and noise reduction. The proposed system aims to suppress noise and reverberation by first employing a minimum variance distortion-less response beamformer, then the beamformer output is processed by a single channel speech enhancement method to suppress the residual noise and reverberation.

Beamformer designs are known to be highly sensitive to mismatches in microphone characteristics such as gain, phase and position or source spreading and local scattering. Any violation in these characteristics can significantly degrade the overall performance [5,8]. Hence, developing a robust beamformer design technique which accounts for arbitrary unknown model mismatch is desirable. In principle it would be possible to calibrate each microphone as well as the combined array. However, the drawbacks of calibration are: firstly, microphone characteristics change over time which means that calibration does not provide a long term solution, secondly, they are time consuming as every individual microphone as well as the combined array is required to be calibrated. Several robust broadband beamformer designs have been proposed in recent years using different techniques. In [30], a robust beamforer design proposed by imposing a constraint on the the norm of the cost function. In such technique, significant improvement in the robustness of the beamformenr response and the sidelobe attenuation is achieved. Another robust beamformer technique is achieved by considering the microphone characteristics in the beamformer design procedure, either by using the mean performance optimization [8,13, 16] or the worst case optimization method [4].

The aim of this paper is to extend the indoor beamforming design [16] by including robustness towards the microphone characteristics (gain and phase) into the design. Specifically, the mean performance of the designed beamformer for all possible microphone characteristics according to a given distribution and uncertainty has been developed. In [18] the robust broadband beamformer is formulated using a multiplicative uncertainty model, whereas in this paper we consider an additive error model instead. The beamformer design methods that have been considered in this study are:

i Design using direct path only of the RIR.
ii Robust design using direct path.

iii Using RIR based on the Image Source Method (ISM) with a specific rever-
    beration time.
iv Robust Indoor beamformer design which combines steps ii and iii.

The aforementioned beamformer designs are examined for different acous-
tically adverse environments using simulated and measured room impulse re-
sponses. Evaluation results from the four designs show that robust direct path
based beamformer can achieve almost the same performance of indoor beam-
former design under different reverberant environments despite being a much
simpler and faster design method. Moreover, robust direct design shows robust-
ness in the beamformer response in presence of local scattering perturbation.
In addition, the robust indoor design provides stronger robustness towards
combinations of reverberation and microphone perturbations in amplitude and
phase.

This paper is organized as follows: In Section 2 the problem is formu-
lated. Section 3 describes indoor broadband beamformer design problem as
WLS problem where RIR is simulated using ISM room simulator. Section
4 demonstrates the robust broadband beamformer design using mean per-
formance optimization method and by using additive error model. Section 5
discusses the aperture size optimization problem while Section 6 outlines the
objective measurements used for performance evaluation. Section 7 presents
evaluation results and Section 8 concludes the paper.

## 2 Problem formulation

First, we consider the case of direct path beamformer design, an M element
microphone array in positions $\mathbf{r}_m$, $m = 1, 2, \ldots, M$, and an $L$ tap FIR filter
behind each microphone as depicted in Figure 1. Assume $S(f)$ is the spec-
tral density of source signal at position vector $\mathbf{r}$ traveling in a homogeneous
non-dispersive free field. The received microphone signals are sampled syn-
chronously at a rate of $f_s$. The transfer function (Green function) between the
source signal and each microphone array element can be written as

$$R_m(\mathbf{r}, f) = \frac{1}{\|\mathbf{r} - \mathbf{r}_m\|} \exp^{\left(-j2\pi f \frac{\|\mathbf{r} - \mathbf{r}_m\|}{c}\right)}, \ 1 \leq m \leq M \tag{1}$$

where $f$ is the frequency and $c = 340.9 \ m/s$ denotes the speed of sound. The
array response vector can be obtained by combining the transfer function from
the source to each microphone element with FIR filter response

$$\mathbf{d}(\mathbf{r}, f) = \mathbf{R}(\mathbf{r}, f) \otimes \mathbf{d}_0(f) \tag{2}$$

where $\otimes$ denotes for the Kronecker product, $\mathbf{R}(\mathbf{r}, f) = [R_1(\mathbf{r}, f), \ldots \ldots, R_M(\mathbf{r}, f)]^T$
and $\mathbf{d}_0(f)$ is the FIR filter response vector,

$$\mathbf{d}_0(f) = \left[1, e^{-j2\pi f/f_s}, \ldots, e^{-j2\pi f(L-1)/f_s}\right]^T \tag{3}$$
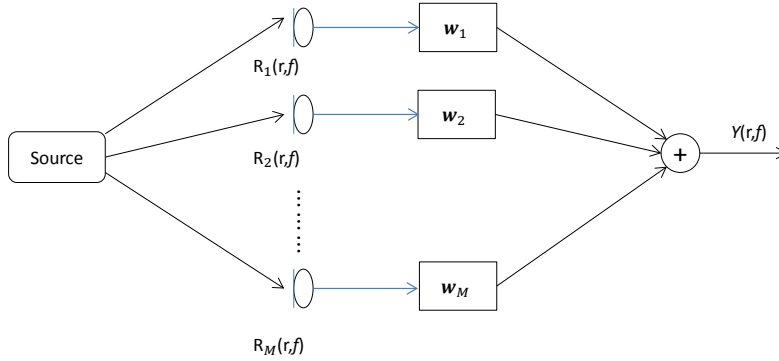
Fig. 1: Block diagram of the broadband beamformer.

and the subscript $(.)^T$ represents the vector transpose. Then, the actual response of the broadband beamformer as a function of frequency $f$ and source position $\mathbf{r}$ is given by

$$G(\mathbf{r}, f) = \mathbf{w}^T \mathbf{d}(\mathbf{r}, f) \qquad (4)$$

where $\mathbf{w}$ denotes the FIR filter coefficients vector of length $ML$ with real values. Then, the beamformer frequency domain output is given by

$$Y(r, f) = G(\mathbf{r}, f)S(f). \qquad (5)$$

## 3 Indoor Broadband Beamformer Design

In the case of indoor beamformer design, a speech source with a microphone array in an indoor room environment are considered according to Fig. 1. The source signal transmitted from the source and received at each microphone element. To model the transmission through a real room, an acoustic room simulator using the image source method (ISM) was used to obtain the room impulse responses (RIRs). The frequency domain room response from the speech source to the microphone array comprises of direct $\mathbf{R}_{dir}(\mathbf{r}, f)$ and reverberant $\mathbf{R}_{rev}(\mathbf{r}, f)$ components. RIR can be written as

$$\mathbf{R}(\mathbf{r}, f) = \mathbf{R}_{dir}(\mathbf{r}, f) + \mathbf{R}_{rev}(\mathbf{r}, f). \qquad (6)$$

In general, the broadband beamformer design problem is to calculate the filter coefficients $\mathbf{w}$ such that the actual response $G(\mathbf{r}, f)$ optimally fits the desired response $G_d(\mathbf{r}, f)$, which is specified depending on the application with

$$G_d(\mathbf{r}, f) = \begin{cases} e^{-j2\pi f\left(\frac{\|\mathbf{r}-\mathbf{r_c}\|}{c} + \frac{L-1}{2}T\right)}, & \forall (\mathbf{r}, f) \in \mathcal{P} \\ 0, & \forall (\mathbf{r}, f) \in \mathcal{S} \end{cases} \qquad (7)$$

where $\mathbf{r}_c$ is the coordinate of the reference microphone. $\mathcal{P}$ and $\mathcal{S}$ represent the passband and the stopband regions, respectively, and $T = 1/f_s$. The problem is to minimize the Weighted Least Square (WLS) error $J_{WLS}(\mathbf{w})$ as

$$J_{WLS}(\mathbf{w}) = \int_{\Omega} \int_{\mathcal{R}} V(\mathbf{r}, f) \left| G(\mathbf{r}, f) - G_d(\mathbf{r}, f) \right|^2 d\mathbf{r} df \qquad (8)$$

where $\mathcal{R}$ and $\Omega$ denote the space and frequency domain, respectively. $V(\mathbf{r}, f)$ represents a positive weighting function. Since the reverberation path is part of the room impulse response as in Eq. (8), it cannot be controlled directly [16]. Thus, a modified design problem that includes the deviation from the direct path with the desired frequency response and the error due to the reverberation path is desirable, as follows

$$
\begin{aligned}
J_{mod,WLS}(\mathbf{w}) =& \int_{\Omega} \int_{\mathcal{R}} (V_1(\mathbf{r}, f) \left| G_{dir}(\mathbf{r}, f) - G_d(\mathbf{r}, f) \right|^2 \\
& + V_2(\mathbf{r}, f) \left| \mathrm{G}_{rev}(\mathbf{r}, f) \right|^2) d\mathbf{r} df \\
=& \int_{\Omega} \int_{\mathcal{R}} (V_1(\mathbf{r}, f) \left| \mathbf{w}^T \mathbf{d}_{dir}(\mathbf{r}, f) - G_d(\mathbf{r}, f) \right|^2 \\
& + V_2(\mathbf{r}, f) \left| \mathbf{w}^T \mathbf{d}_{rev}(\mathbf{r}, f) \right|^2) d\mathbf{r} df,
\end{aligned}
$$

where $V_1(\mathbf{r}, f)$ and $V_2(\mathbf{r}, f)$ are positive weighting functions. In order to simplify the above cost function, it can be transformed to a quadratic cost function,

$$J_{mod,WLS}(\mathbf{w}) = \mathbf{w}^T \mathbf{Q}_{mod,WLS} \mathbf{w} - 2\mathbf{p}_{mod,WLS}^T \mathbf{w} + const \qquad (9)$$

where

$$
\begin{aligned}
\mathbf{Q}_{mod,WLS} =& \int_{\Omega} \int_{\mathcal{R}} (V_1(\mathbf{r}, f) \Re \left\{ \mathbf{d}_{dir}(\mathbf{r}, f) \mathbf{d}_{dir}^H(\mathbf{r}, f) \right\} \\
& + V_2(\mathbf{r}, f) \Re \left\{ \mathbf{d}_{rev}(\mathbf{r}, f) \mathbf{d}_{rev}^H(\mathbf{r}, f) \right\}) d\mathbf{r} df \\
\mathbf{p}_{mod,WLS} =& \int_{\Omega} \int_{\mathcal{R}} V_1(\mathbf{r}, f) \Re \left\{ \mathbf{d}_{dir}(\mathbf{r}, f) G_d^H(\mathbf{r}, f) \right\} d\mathbf{r} df \\
const =& \int_{\Omega} \int_{\mathcal{R}} V_1(\mathbf{r}, f) \left| G_d(\mathbf{r}, f) \right|^2 d\mathbf{r} df
\end{aligned}
$$

and $\mathbf{d}_{dir}(\mathbf{r}, f) = \mathbf{R}_{dir}(\mathbf{r}, f) \otimes \mathbf{d}_0(f)$, $\mathbf{d}_{rev}(\mathbf{r}, f) = \mathbf{R}_{rev}(\mathbf{r}, f) \otimes \mathbf{d}_0(f)$. The optimal filter coefficients vector that minimizes $J_{mod,WLS}(\mathbf{w})$ is obtained by

$$\mathbf{w} = \mathbf{Q}_{mod,WLS}^{-1} \mathbf{p}_{mod,WLS}. \qquad (10)$$

## 4 Robust Beamformer Design

Broadband beamformers designed with Minimax or WLS techniques are highly sensitive to errors in microphone characteristics such as gain, phase and position [8]. Any violation from the assumed characteristics can significantly degrade the overall performance. Thus, for practical applications it is important to consider robustness in the beamformer design procedure. In this work, we employ a stochastic additive error model to microphone characteristics error (gain and phase) [22]. Assuming random model errors denoted by $\mathbf{a}_{dir}(\mathbf{r}, f)$ and $\mathbf{a}_{rev}(\mathbf{r}, f)$ for the direct and the reverberation parts, respectively. The $m^{th}$ microphone in the model error vector can be characterized by the gain errors $|\mathbf{a}_{dir}(\mathbf{r}, f)|$, $|\mathbf{a}_{rev}(\mathbf{r}, f)|$ and the phase errors $\arg(\mathbf{a}_{dir}(\mathbf{r}, f))$, $\arg(\mathbf{a}_{rev}(\mathbf{r}, f))$. Accordingly, the perturbed response vectors are given by

$$
\begin{aligned}
\tilde{\mathbf{R}}_{dir}(\mathbf{r}, f) &= \mathbf{R}_{dir}(\mathbf{r}, f) + \mathbf{a}_{dir}(\mathbf{r}, f) \\
\tilde{\mathbf{R}}_{rev}(\mathbf{r}, f) &= \mathbf{R}_{rev}(\mathbf{r}, f) + \mathbf{a}_{rev}(\mathbf{r}, f).
\end{aligned}
\tag{11}
$$

Following from (2), the perturbed array response vector is given by

$$
\begin{aligned}
\tilde{\mathbf{d}}_{dir}(\mathbf{r}, f) &= \tilde{\mathbf{R}}_{dir}(\mathbf{r}, f) \otimes \mathbf{d}_0(f) \\
&= (\mathbf{a}_{dir}(\mathbf{r}, f) \otimes \mathbf{d}_0(f)) + \mathbf{d}_{dir}(\mathbf{r}, f)
\end{aligned}
\tag{12}
$$

and

$$
\tilde{\mathbf{d}}_{rev}(\mathbf{r}, f) = (\mathbf{a}_{rev}(\mathbf{r}, f) \otimes \mathbf{d}_0(f)) + \mathbf{d}_{rev}(\mathbf{r}, f)
$$

$$
\begin{aligned}
\tilde{\mathbf{Q}}_{dir}(\mathbf{r}, f) &= \tilde{\mathbf{d}}_{dir}(\mathbf{r}, f)\tilde{\mathbf{d}}_{dir}^H(\mathbf{r}, f) \\
&= (\mathbf{a}_{dir}(\mathbf{r}, f) \otimes \mathbf{d}_0(f) + \mathbf{d}_{dir}(\mathbf{r}, f)) \\
&\quad \times (\mathbf{a}_{dir}(\mathbf{r}, f) \otimes \mathbf{d}_0(f) + \mathbf{d}_{dir}(\mathbf{r}, f))^H \\
&= \mathbf{Q}_{dir}(\mathbf{r}, f) + (\mathbf{a}_{dir}(\mathbf{r}, f)\mathbf{a}_{dir}^H(\mathbf{r}, f) + \mathbf{a}_{dir}(\mathbf{r}, f)\mathbf{R}_{dir}^H(\mathbf{r}, f) \\
&\quad + \mathbf{R}_{dir}(\mathbf{r}, f)\mathbf{a}_{dir}^H(\mathbf{r}, f)) \otimes \mathbf{d}_0(f)\mathbf{d}_0^H(f)
\end{aligned}
\tag{13}
$$

$$
\begin{aligned}
\tilde{\mathbf{Q}}_{rev}(\mathbf{r}, f) &= \tilde{\mathbf{d}}_{rev}(\mathbf{r}, f)\tilde{\mathbf{d}}_{rev}^H(\mathbf{r}, f) \\
&= (\mathbf{a}_{rev}(\mathbf{r}, f) \otimes \mathbf{d}_0(f) + \mathbf{d}_{rev}(\mathbf{r}, f)) \\
&\quad \times (\mathbf{a}_{rev}(\mathbf{r}, f) \otimes \mathbf{d}_0(f) + \mathbf{d}_{rev}(\mathbf{r}, f))^H \\
&= \mathbf{Q}_{rev}(\mathbf{r}, f) + (\mathbf{a}_{rev}(\mathbf{r}, f)\mathbf{a}_{rev}^H(\mathbf{r}, f) + \mathbf{a}_{rev}(\mathbf{r}, f)\mathbf{R}_{rev}^H(\mathbf{r}, f) \\
&\quad + \mathbf{R}_{rev}(\mathbf{r}, f)\mathbf{a}_{rev}^H(\mathbf{r}, f)) \otimes \mathbf{d}_0(f)\mathbf{d}_0^H(f)
\end{aligned}
\tag{14}
$$

where $\mathbf{Q}_{dir}(\mathbf{r}, f) = \mathbf{d}_{dir}(\mathbf{r}, f)\mathbf{d}_{dir}^H(\mathbf{r}, f)$ and $\mathbf{Q}_{rev}(\mathbf{r}, f) = \mathbf{d}_{rev}(\mathbf{r}, f)\mathbf{d}_{rev}^H(\mathbf{r}, f)$.

$$
\begin{aligned}
\tilde{\mathbf{p}}_{dir} &= \tilde{\mathbf{d}}_{dir}(\mathbf{r}, f)G_d^H(\mathbf{r}, f) \\
&= \mathbf{p}_{dir}(\mathbf{r}, f)) + (\mathbf{a}_{dir}(\mathbf{r}, f) \otimes \mathbf{d}_0(f))G_d^H(\mathbf{r}, f)
\end{aligned}
\tag{15}
$$

where $\mathbf{p}_{dir}(\mathbf{r}, f) = \mathbf{d}_{dir}(\mathbf{r}, f)G_d^H(\mathbf{r}, f)$. Let $\mathbf{\Xi}_{dir}$ a random matrix that envolves the perturbation elements for the direct path,

$$\mathbf{\Xi}_{dir} = \mathbf{a}_{dir}\mathbf{a}_{dir}^H. \tag{16}$$

From now on, the term $(\mathbf{r}, f)$ is dropped from $\mathbf{a}_{dir}$ for notational convenience. Since we aim to use mean performance optimization technique by using probability density function of the gain and phase

$$\bar{\mathbf{\Xi}}_{dir} = E\left[\mathbf{\Xi}_{dir}\right] = E\left[\mathbf{a}_{dir}\mathbf{a}_{dir}^H\right] \tag{17}$$
$$= \int_{a_1}\cdots\int_{a_M} \mathbf{\Xi}_{dir} f_{\Xi}(a_1)...f_{\Xi}(a_M)da_1\cdots da_M$$

and

$$\bar{\mathbf{a}}_{dir} = E\left[\mathbf{a}_{dir}\right] \tag{18}$$
$$= \int_{a_1}\cdots\int_{a_M} \mathbf{a}_{dir} f_{\Xi}(a_1)...f_{\Xi}(a_M)da_1\cdots da_M.$$

where $f_{\Xi}(a_m)$, $1 \le m \le M$, is the PDF for $m^{th}$ sensor's errors. In order to simplify the design problem we assume that each sensor's error is independent of frequency and space. Then, using expectation on equations (13) to (15) we obtain

$$\bar{\mathbf{Q}}_{dir}(\mathbf{r}, f) = E\left[\tilde{\mathbf{Q}}_{dir}(\mathbf{r}, f)\right] \tag{19}$$
$$= (\bar{\mathbf{\Xi}}_{dir} + \bar{\mathbf{a}}_{dir}\mathbf{R}_{dir}^H(\mathbf{r}, f) + \mathbf{R}_{dir}(\mathbf{r}, f)\bar{\mathbf{a}}_{dir}^H) \otimes \mathbf{d}_0(f)\mathbf{d}_0^H(f) + \mathbf{Q}_{dir}(\mathbf{r}, f),$$

$$\bar{\mathbf{Q}}_{rev}(\mathbf{r}, f) = E\left[\tilde{\mathbf{Q}}_{rev}(\mathbf{r}, f)\right] \tag{20}$$
$$= ((\bar{\mathbf{\Xi}}_{rev} + \bar{\mathbf{a}}_{rev}\mathbf{R}_{rev}^H(\mathbf{r}, f) + \mathbf{R}_{rev}(\mathbf{r}, f)\bar{\mathbf{a}}_{rev}^H) \otimes \mathbf{d}_0(f)\mathbf{d}_0^H(f)) + \mathbf{Q}_{rev}(\mathbf{r}, f)$$

and

$$\bar{\mathbf{p}}_{dir}(\mathbf{r}, f) = E\left[\tilde{\mathbf{p}}_{dir}(\mathbf{r}, f)\right] \tag{21}$$
$$= (\bar{\mathbf{a}}_{dir} \otimes \mathbf{d}_0(f))G_d^H(\mathbf{r}, f) + \mathbf{p}_{dir}(\mathbf{r}, f).$$

For simplicity, assuming that the error model for the direct path and the reverberation part are the same. Thus we have,

$$\bar{\mathbf{\Xi}}_{dir} = \bar{\mathbf{\Xi}}_{rev} = \bar{\mathbf{\Xi}}. \tag{22}$$

The robust weighted least square error can be given as

$$J_{mod,WLS,rb}(\mathbf{w}) = \mathbf{w}^T\bar{\mathbf{Q}}_{rb}\mathbf{w}_{rb} - 2\bar{\mathbf{p}}_{rb}^T\mathbf{w}_{rb} + const \tag{23}$$

where

$$\bar{\mathbf{Q}}_{rb} = \int\limits_{\Omega}\int\limits_{\mathcal{R}} (V_1(\mathbf{r}, f)\Re\left\{\bar{\mathbf{Q}}_{dir}(\mathbf{r}, f)\right\} + V_2(\mathbf{r}, f)\Re\left\{\bar{\mathbf{Q}}_{rev}(\mathbf{r}, f)\right\})d\mathbf{r}df.$$

$$\bar{\mathbf{p}}_{rb} = \int\limits_{\Omega}\int\limits_{\mathcal{R}} V_1(\mathbf{r}, f)\Re\left\{\bar{\mathbf{p}}_{dir}(\mathbf{r}, f)\right\}d\mathbf{r}df.$$

The design of robust beamformer can be obtained by

$$\mathbf{w}_{rb} = \bar{\mathbf{Q}}_{rb}^{-1}\bar{\mathbf{p}}_{rb}. \tag{24}$$

## 5 Aperture Size Optimization

So far the formulation of the beamformer design problem has only considered one specific array size and configuration as in Eq. (8). But it is well established that there is an impact of array aperture size on the design performance. Different aperture size can lead to different array resonse [9,27]. Hence, it is important to consider the array aperture size problem for the overall performance. Beamformer design problem in this case can be formulated as a minimization of cost function with respect to filter coefficients $\mathbf{w}$ and interelement space between adjacent microphones ($d$) which can be written as [13]

$$J_{\text{WLS,opt}}(\mathbf{w}, d) = \int\limits_{\Omega}\int\limits_{\mathcal{R}} V(\mathbf{r}, f)\left|G(\mathbf{r}, f, d) - G_d(\mathbf{r}, f)\right|^2 d\mathbf{r}df \tag{25}$$

This problem can be solved by combining Weighted Least Square and Golden Section Search optimization techniques, by first optimizing the cost function with respect to $\mathbf{w}$ while searching for the optimal interelement space ($d$). Algorithm 1 shows how this combined optimization has been performed.

Step 1: Initialize an interval $[d_l, d_u]$ and *tol* sufficiently small
Step 2: Set the golden ratio $\varphi = (\sqrt{5} - 1)/2$
Step 3: Set intermediate points, $a = d_u - \varphi * (d_u - d_l)$ and
 $b = d_l + \varphi * (d_u - d_l)$
Step 4: Evaluate the function at the intermediate points
 $f(a) = J_{\text{WLS}}(a)$ and $f(b) = J_{\text{WLS}}(b)$
Step 5: **While** $((a - b) > tol)$, number
     **If** $f(a) < f(b)$ then update the intermediate points
      $[d_u = b]$ ,$[b = a]$ and $a = d_u - \varphi * (d_u - d_l)$
     **else**
      $[d_l = a]$, $[a = b]$ and $b = d_l + \varphi * (d_u - d_l)$
     **end**
Step 6: Evaluate the functions in the updated points
     **end**
Step 7: The minimum occurs at $d = (d_u + d_l)/2$

**Algorithm 1:** Array aperture size optimization algorithm

## 6 Objective Measurements

There are different objective measurements in the literature to evaluate the performance of the beamformer designs. For dereverberation performance, objective measurements can be classified into two categories: channel based measurement [14] and signal based measurement [19]. In this paper, for the channel based measurment, we used direct to reverberant ratio measurement to evaluate the dereverberation ability of the designed beamformers. The direct to reverberant ratio, DRR, is defined as follows [20]

$$\text{DRR} = 20 \log 10 \frac{\text{DRR}_{out}}{\text{DRR}_{in}} \, [\text{dB}].\tag{26}$$

Here,

$$\text{DRR}_{out} = \frac{\left\| \mathbf{w}^T \mathbf{d}_{dir}(\mathbf{r}, f) \right\|_2^2}{\left\| \mathbf{w}^T \mathbf{d}(\mathbf{r}, f) - \mathbf{w}^T \mathbf{d}_{dir}(\mathbf{r}, f) \right\|_2^2}\tag{27}$$

$$\text{DRR}_{in} = \frac{\left\| \mathbf{1}^T \mathbf{R}_{dir}(\mathbf{r}, f) \right\|_2^2}{\left\| \mathbf{1}^T (\mathbf{R}(\mathbf{r}, f) - \mathbf{R}_{dir}(\mathbf{r}, f)) \right\|_2^2}\tag{28}$$

where $\mathbf{1}$ is an $M$ element vector with ones and $||(\cdot)||_2^2$ denotes $\int\int_{\mathcal{P}} |(\cdot)|^2 \, d\mathbf{r} df$, $\forall (\mathbf{r}, f) \in \mathcal{P}$ where $\mathcal{P}$ is the passband region.

For the signal based measurement, segmental signal to noise and reverberation ratio SSNRR is used to measure the speech distortion because of noise and reverberation [29]. It can be formulated as

$$\text{SSNRR}_{seg} = \frac{1}{N_{seg}} \sum_{l=0}^{N_{seg}-1} 10 \log 10 \left( \frac{\| \mathbf{s}_d(l) \|^2}{\| s_d(l) - \mathbf{y}(l) \|^2} \right) \, [\text{dB}]\tag{29}$$

where $\mathbf{s}_d(l)$ represents desired signal, $y(l)$ represents the estimated speech from the beamformer output, and $N_{seg}$ denotes the number of signal segments. This is obtained by computing desired and estimated signals as short overlapping signal segments and then an average of SSNRR values in dB is taken over all segments. Moreover, to test the overall suppression performance in the stopband region, signal suppression measurement is used as follows [16]

$$\text{SUPP} = 10\log 10 \frac{\|S(f)\|_2^2}{\|Y(f)\|_2^2} \tag{30}$$

where $S(f)$ and $Y(f)$ denote the frequency spectrum of the input signal and the output signal , respectively. Furthermore, $\|(\cdot)\|_2^2$ denotes $\int_{\mathcal{F}} |(\cdot)|^2 \, df, \, \forall f \in \mathcal{F}$ where $\mathcal{F}$ is the passband region.

## 7 Design Examples

This section presents a number of design examples with the aim to verify the beamformer design formulations in Section 3 (indoor beamformer design) and Section 4 (robust beamformer design) using simulated data (room impulse response) and real data. The parameters used in the simulation is given in Table 6. Those are the parameter values used unless otherwise specified. The frequency domain expression of the room impulse response is computed using Equation (6). As a special case, direct path based beamformer is designed by using Equation (6) with a reverberation time $T_{60} = 0\,s$, i.e. room response consists of direct path response only. Whereas, indoor beamformers are designed with reverberation time $T_{60} = 0.2\,s$

Equation (10) is used for direct path and indoor beamformer designs. For robust direct path and indoor beamformer design examples, mean performance optimization method is used with amplitude and phase variation both following a uniform distribution with intervals $[\pm 10\% \, \mathbf{R}(\mathbf{r}, f)]$ and [-0.1 rad, 0.1 rad], respectively. Equation (11) is used as the perturbed response and Equation (24) is used for the beamformer design. The designed beamformers were tested using simulated room impulse response from room acoustic simulator based on the ISM method [2,15]. We define a simple rectangular room with dimensions $4m \times 8m \times 3m$ and uniform absorption coefficients characterizing the room surfaces. The passband region is given as

$$\mathcal{P} = \{x = 1m, \ 3.5m \leq y \leq 4.5m, \ z = 1m, \ 200kHz \leq f \leq 3800Hz\}$$

while the stop band region is

$$\mathcal{S} = \{x = 1m, \ 3.5m \leq y \leq 4.5m, \ z = 1m, \ 3850Hz \leq f \leq 4kHz\}$$
$$\cup \{x = 1m, 1m \leq y \leq 2.5m \cup 5.5m \leq y \leq 7m, z = 1m, \ 100Hz \leq f \leq 4000Hz\}.$$

Different scenarios are presented to evaluate the designed beamformers. First, the cost function and the beampattern performances in varying reverberant

environments are evaluated, then the suppression performance in stopband region for different reverberation conditions are evaluated, finally, the joint de-reverberation and noise suppression performance in environments which included both noise and reverberation are evaluated using estimated Room Impulse Response (RIR) or measured (RIR) [12].

## 7.1 Overall performance and cost function evaluation for different reverberation time

The four design methods are evaluated by calculating the amplitude response of the overall beamformer including the room response according to Equation (4) as a function of spatial coordinate and frequency. The designs have been evaluated for $T_{60} = 0.1\,s$ and $T_{60} = 0.2\,s$.

Fig. 2 shows the magnitude frequency response of direct path and robust direct beamformer designs applied for different reverberation time. Similarly, Fig. 3 shows the magnitude frequency response of indoor design and robust indoor design applied for different reverberation time. It can be seen from the figures that the robust direct path beamformer design has a similar performance as the indoor design response while the direct path beamformer response performance deteriorates in the presence of the reverberation. As such a simple robust direct path beamformer can be employed to the indoor applications as it can achieve approximately the same performance as the indoor beamformer design while having a significantly lower computational complexity as the reverberation part is not included.

Table 1 shows the values of cost function in Equation (8) for different design methods. We evaluate the cost function for different reverberation times using the optimal weights with $T_{60} = 0\,s$ and $T_{60} = 0.2\,s$ for different design methods to get an impression of the sensitivity of the cost function for changing reverberation times. It can be seen from Table 1 that the cost function of the robust direct design follows a similar trend as the indoor beamformer, whereas the cost function of the direct design increased significantly with increasing reverberation time.

## 7.2 Dereverberation performance

In this section, we evaluated the performance of the designed beamformers in terms of DRR for different source distance and number of microphones while the distance between the microphones remained constant. We assume a noise free reverberant environment at $T_{60} = 0.2\,s$. The results that were obtained by the robust direct design is similar to the results obtained by the indoor designs, which are much higher than the DRR that was obtained by the direct design. The direct to reverberant ratio has been studied as a function of the distance between the desired source and the microphone array as depicted in Fig. 4 (left side). It can be clearly seen that direct to reverberant ratio
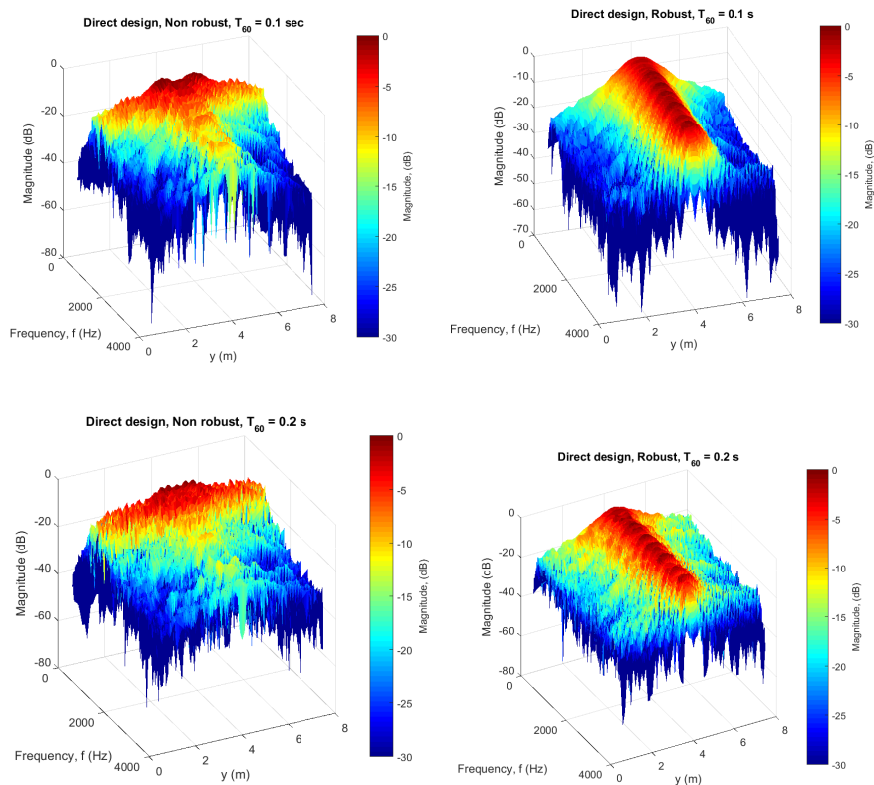
Fig. 2: Magnitude response of direct beamformer and robust direct beamformer under different reverberation time.

| $T_{60}(s)$ | Cost function of Direct Path beamformer design (dB) | Cost function of Robust Direct Path beamformer design (dB) | Cost function of Indoor beamformer design (dB) | Cost function of Robust Indoor beamformer design (dB) |
|---|---|---|---|---|
| 0.1 | -7.53 | -23.22 | -23.29 | -20.98 |
| 0.15 | -2.13 | -20.56 | -22.02 | -20.24 |
| 0.2 | 1.07 | -18.50 | -20.80 | -19.43 |
| 0.25 | 3.35 | -16.98 | -19.76 | -18.68 |
| 0.3 | 5.08 | -15.79 | -18.22 | -17.98 |
| 0.35 | 7.53 | -14.69 | -17.32 | -16.76 |

Table 1: Comparison of the cost function for different reverberation times for the direct design and the robust direct design ($T_{60} = 0\,s$), the indoor design and the indoor robust design ($T_{60} = 0.2\,s$).
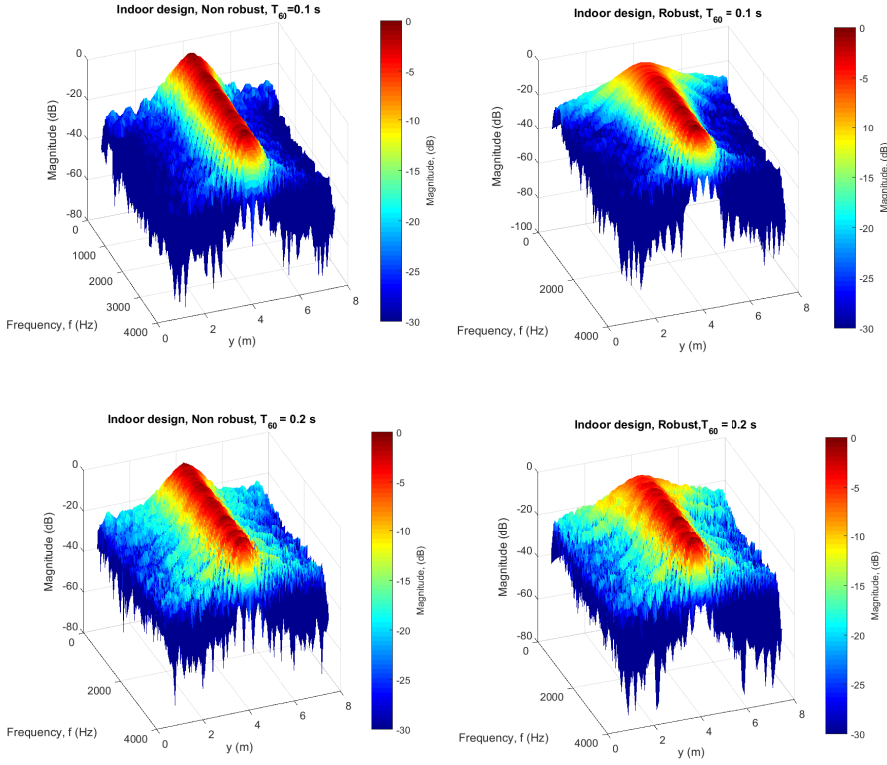
Fig. 3: Magnitude response of indoor beamformer and robust indoor beamformer under different reverberation time.

results that are obtained by the indoor designs and robust direct design are almost not affected by the source to microphone array distance. Moreover, DRR has been studied as a function of the number of microphones as shown in Fig. 4 (right side), significant improvements in DRR with growing number of microphone elements are obtained by the indoor designs and the robust direct design. Whereas, the direct design does not show any improvement.

### 7.3 Suppression performance in stopband region

In this section, we present a comparison of the interference suppression capabilities of the designed beamformers under different reverberation conditions. We use a female speech signal as an interference in the stopband region from position $= (1, 6, 1)$ m. Table 2 shows the amplitude suppression results obtained from the different designed beamformers under varying reverberation times. It can be clearly observed that the indoor designs perform better than
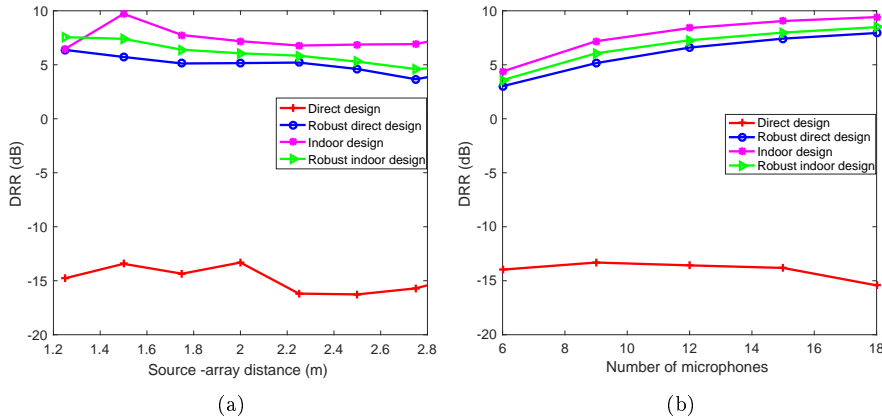
Fig. 4: Direct to reverberant ration performance under (a) different source-microphone array distance, (b) different number of microphones.

| $T_{60}(s)$ | SUPP of Direct Path beamformer design (dB) | SUPP of Robust Direct Path beamformer design (dB) | SUPP of Indoor beamformer design (dB) | SUPP Robust Indoor beamformer design (dB) |
|---|---|---|---|---|
| 0.1 | -4.952 | 12.184 | 14.244 | 14.648 |
| 0.15 | -5.989 | 10.247 | 12.579 | 13.323 |
| 0.2 | -6.976 | 9.031 | 11.323 | 12.224 |
| 0.25 | -7.271 | 8.210 | 10.401 | 11.389 |
| 0.3 | -8.292 | 7.600 | 9.685 | 10.737 |
| 0.35 | -8.750 | 7.113 | 9.112 | 10.206 |

Table 2: Comparison results among direct path based beamformer and its robust design ($T_{60} = 0\,s$), indoor beamformer and its robust design ($T_{60} = 0.2\,s$) on the interference suppression at different reverberation time.

the direct design. Moreover, the robust direct design follows the same trend as the indoor design under different reverberation conditions. This demonstrates the suppression capability of the robust direct design in reverberant conditions.

## 7.4 Joint dereverberation and noise suppression performance

Now the combined dereverberation and noise reduction performance for the designed beamformers are evaluated in terms of segmental signal to noise and reverberation ratio (SSNRR) [?], which is a measure of the distortion occurs due to the interference (noise and reverberation). The reverberant signals are

generated using simulated room impulse response and measured room impulse response.

In this example, a linear microphone array with 8 elements with inter-element space of 0.08 m is placed in a reverberant room of size $(6m \times 6m \times 2.4m)$ with variable reverberation time $T_{60} = 0.16\,s$ and $T_{60} = 0.36\,s$. The desired speaker is 1 m from the microphone array at angle $0°$ and the noise source is 1 m from the microphone array at angle $90°$. The room setup is depicted in Fig. 5. Different beamformer designs are tested both in simulated and real room environments. The noisy environment consists of reverberation and directional white noise source (jammer) with varied SJR levels (10-30 dB).

In the simulated room scenario, room impulse response is generated using image source method (ISM) [2,15]. The reverberant signals received by the microphone array are obtained by convolving the simulated RIR with the source signal. For the real room environment evaluation, we used measured room impulse responses (RIR) [12]. The reverberant signals received by the microphone array are generated by convolving the speech signals with the measured room impulse response.

Fig. 6 shows the results for the SSNRR using simulated RIR (left side) and measured RIR (right side) under different reverberation time values $T_{60} = 0.16\,s$ and $T_{60} = 0.36\,s$. From the simulated results, it can be clearly observed that the SSNRR results that are obtained by the indoor design and the direct designs are almost identical at $T_{60}=0.16$ sec. In higher reverberation time $T_{60} = 0.36\,s$ the SSNRR results that are obtained by the indoor designs and the robust direct design are much higher than those obtained by the direct design. The SSNRR results that are obtained by using measured RIR show that robust direct design performs almost identical as the indoor design and better than the direct design under low reverberation time $T_{60} = 0.16\,s$. Moreover, robust indoor beamformer design shows significantly better results compared to direct designs and indoor design. However, for $T_{60} = 0.36\,s$ case, although robust direct design shows similar results to direct design in SJR level$< 10$ dB, SSNRR starts to increase at SJR level $> 15$ dB. For higher reverberation time such as, $T_{60} = 0.61\,s$ case, it can be noticed that the indoor designs achieve better performance than the direct designs.

## 7.5 Sensitivity test of beamformer designs

### 7.5.1 Perturbation in microphone characteristics

The next evaluation is on the sensitivity of the designed beamformers against gain and phase mismatches in microphone characteristics. This evaluation is done by performing a Monte-Carlo simulation of the gain and the phase mismatches and evaluate the cost function with fix beamformer coefficients for each simulation round. In Fig. 7 the cost function distribution for the different beamformer designs in form of histograms are presented: (i) non-robust and robust direct path based beamformer with $T_{60} = 0\,s$ and (ii) non-robust and
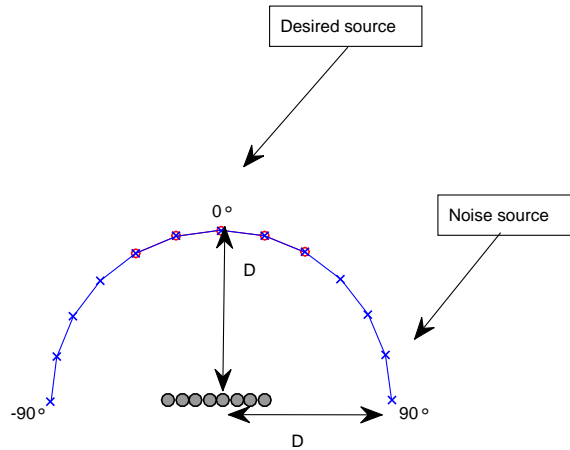
Fig. 5: Room setup with a linear microphone array.

robust indoor beamformer with $T_{60} = 0.2\,s$ . Robust broadband beamformer is designed using mean performance optimization method. The perturbations on each element are made according to uniform distributions in gain [0.997,1.007] and phase [-0.1,0.1] rad. The cost function values are obtained by averaging 100 Monte-Carlo simulations for gain and phase errors. It can be seen from Fig. 7 that non-robust designs (direct path and indoor) beamformers are sensitive to mismatches in microphone characteristics with the cost function values of non-robust direct path design deviate in the range $(-12.83\,\text{dB}, -5\,\text{dB})$, and the cost function values of non-robust indoor design deviate in the range $(-13.22\,\text{dB}, -8.35\,\text{dB})$. On the other hand, the robust direct path and robust indoor design are less sensitive to the mismatches in microphone characteristics as the cost function values deviate significantly less than the non-robust direct path and non-robust indoor designs. Moreover, to investigate the behavior of designed beamformers towards mismatches in microphone characteristics (gain and phase) we calculate the condition number of the correlation matrix $Q$ for the different beamformer designs, as depicted in Table 3. It can be clearly observed that the robust direct path and robust indoor designs have significantly lower condition numbers than non-robust direct path and indoor beamformer designs. As such, the robust direct path and robust indoor designs are significantly less sensitive against errors in microphone characteristics than the direct path and indoor designs.

### 7.5.2 Evaluation for local scattering

In this section, an evaluation of the robustness towards local scattering is presented for all four design methods. In order to simulate local scattering we
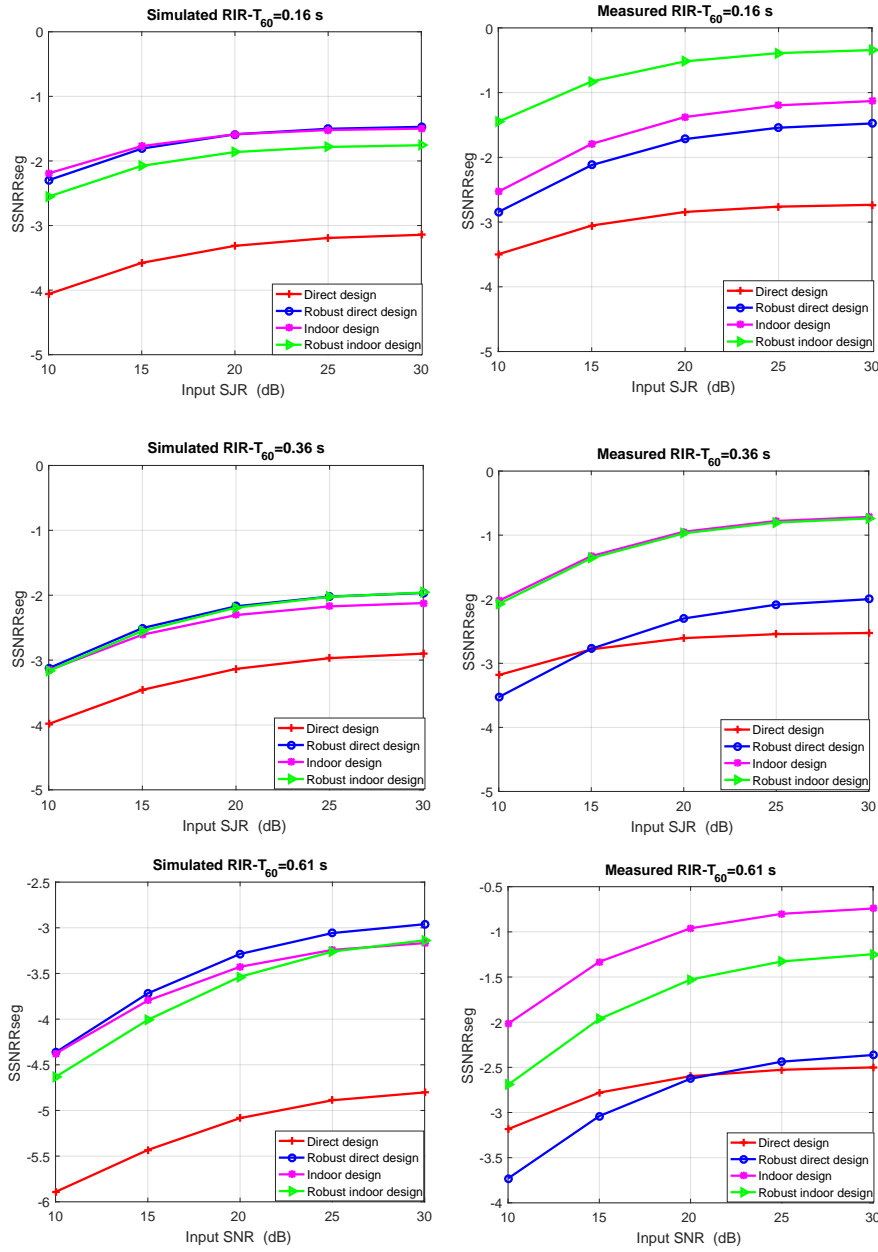
Fig. 6: SSNRR results obtained for different beamformer designs for varying SJR's and reverberation times. The reverberant signals were generated using simulated RIR (left side) and measured RIR (right side) with different reverberation time, $T_{60} = 0.16\,s$ (top), $T_{60} = 0.36\,s$ (middle) and $T_{60} = 0.61\,s$ (bottom).
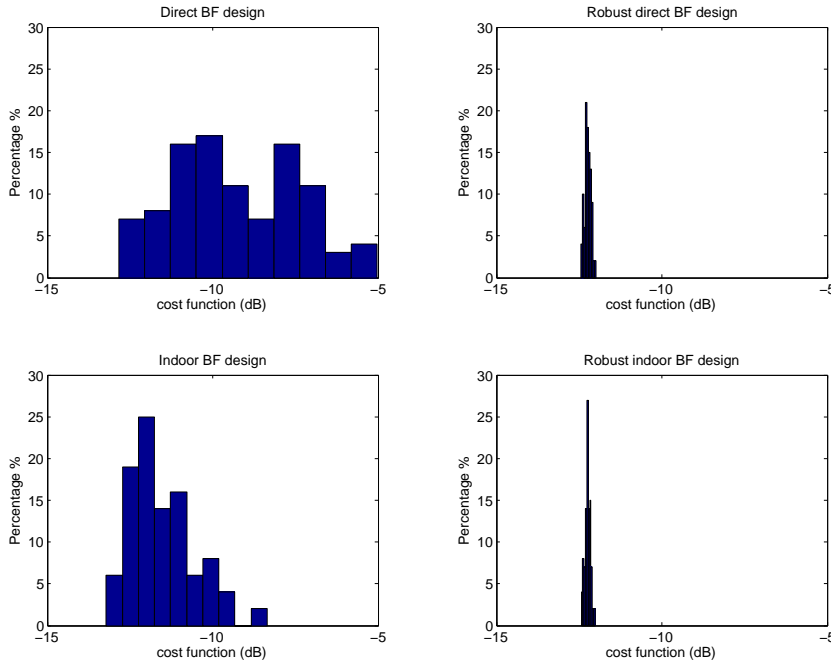
Fig. 7: Histogram of cost function values distribution for different beamformer designs.

| Beamformer design | Condition number of correlation matrix |
|:---:|:---:|
| Direct path | $2.1890e^{17}$ |
| Robust direct path | $1.6265e^{05}$ |
| Indoor | $1.6742e^{17}$ |
| Robust indoor | $1.6873e^{05}$ |

Table 3: Comparison of condition number of correlation matrix among direct path based beamformer and its robust design ($T_{60} = 0\,s$), indoor beamformer and its robust design ($T_{60} = 0.1\,s$).

added 20 additional propagation paths to the direct propagation path, they were simulated using a uniform distribution for the angle of arrival and standard deviation ($-\pi/9, \pi/9$), and gain with Rayleigh distribution and variance (0.01).

Fig. 8 shows the histogram of the cost function for 50 runs. It can be clearly seen that the robust designs demonstrate robustness against perturbed wave propagation compared to the direct design. This demonstrates the efficiency of the indoor designs and robust direct design against local scattering.
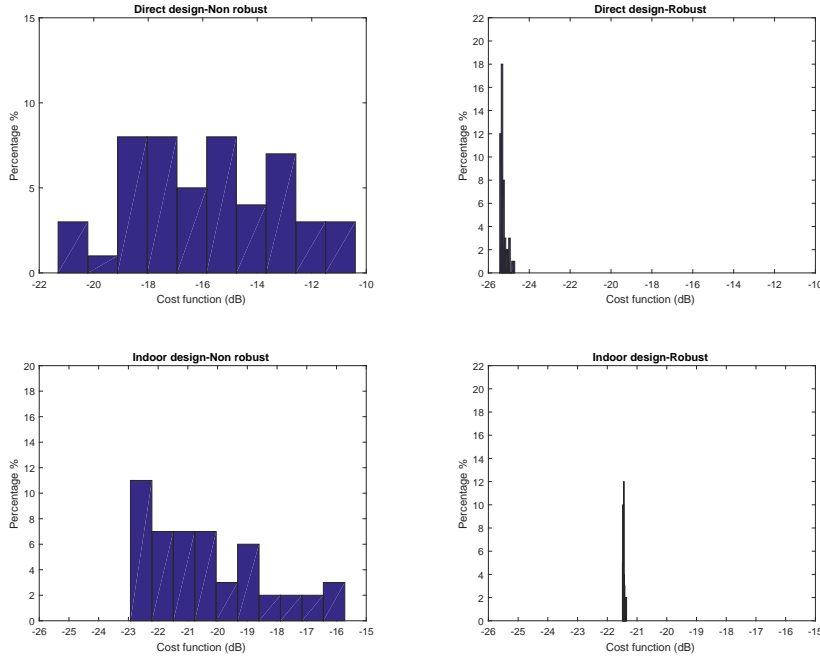
Fig. 8: Histogram of cost function values distribution for different beamformer designs.

## 7.6 Evaluation of calculation time for different beamformer designs

Some applications needs a recalculation of the beamformer weights thus an interesting evaluation to compare is the numerical complexity of the design. Table 4 shows the running time on a I7-4600 CPU 2.1 GHz and 8 Gbyte RAM for the different design methods and the different reverberation times. It can be clearly seen that the running time increase significantly with increasing reverberation time. In addition, the direct design and the robust direct design are significantly faster to calculate compared to the indoor designs.

## 7.7 Results of aperture size optimization

Finally, we study the impact of array aperture size on the design performance as described in Algorithm 1 schedule. The Golden Section Search optimization technique has been used to search for an optimal inter-element spacing between microphones. We investigated all four design methods: (i) direct path $T_{60} = 0\,sec$; (ii) indoor design with $T_{60} = 0.2\,s$; (iii) robust direct path; and (iv)

| Beamformer design | Calculation time (s) |
|---|---|
| Direct path ($T_{60} = 0$) | 4.796 |
| Robust direct path ($T_{60} = 0$) | 23.730 |
| Indoor ($T_{60} = 0.1$) | 38.077 |
| Robust indoor ($T_{60} = 0.1$) | 91.229 |
| Indoor ($T_{60} = 0.2$) | 141.424 |
| Robust indoor ($T_{60} = 0.2$) | 248.767 |
| Indoor ($T_{60} = 0.3$) | 506.926 |
| Robust indoor ($T_{60} = 0.3$) | 736.489 |

Table 4: Calculation time for different beamformer designs.

| Beamformer design | Optimum Inter-element space (m) | Minimum cost function (dB) |
|---|---|---|
| Direct path | 0.110 | -31.977 |
| Robust direct path | 0.115 | -24.557 |
| Indoor | 0.0836 | -21.092 |
| Robust indoor | 0.0873 | -19.173 |

Table 5: Array aperture size optimization for different beamformer designs.

robust indoor design. Table 4 shows the cost function performance of the four different beamformer designs for inter-element spacing ($d$) range from 0.01 m to 0.2 m. It can be seen from the table that the direct beamformer designs have almost the same optimal inter-element space with optimal value (d=-.11 m). While the indoor designs have an optimal interelement space (d=0.08 m). Moreover, the designed beamformers are robust against inter-element spacing as the cost function values deviate only marginally with changing of inter-element spacing as shown in Fig. 7.

## 8 Conclusions and Future Work

In this paper we have included robustness towards microphone characteristics (gain and phase) into the direct design and the indoor design. The indoor design method employs a decomposition of the RIR into a direct path and reverberant path. To calculate the RIR, we have employed the ISM simulator. Numerical results show that robust direct path beamformer can achieve approximately the same performance as indoor beamformer design with a significantly lower computational complexity. Also, the robust direct path design is less sensitive to mismatches in microphone characteristics (gain and phase) than the indoor beamformer design. In addition, robust direct design is also robust to aperture size changes and follows the same trend as the indoor beamformer design. One interesting topic for future work is extending the design formulation to a steerable robust direct design. Moreover, for further investigations different optimization criteria can be used as well as sparse formulations.
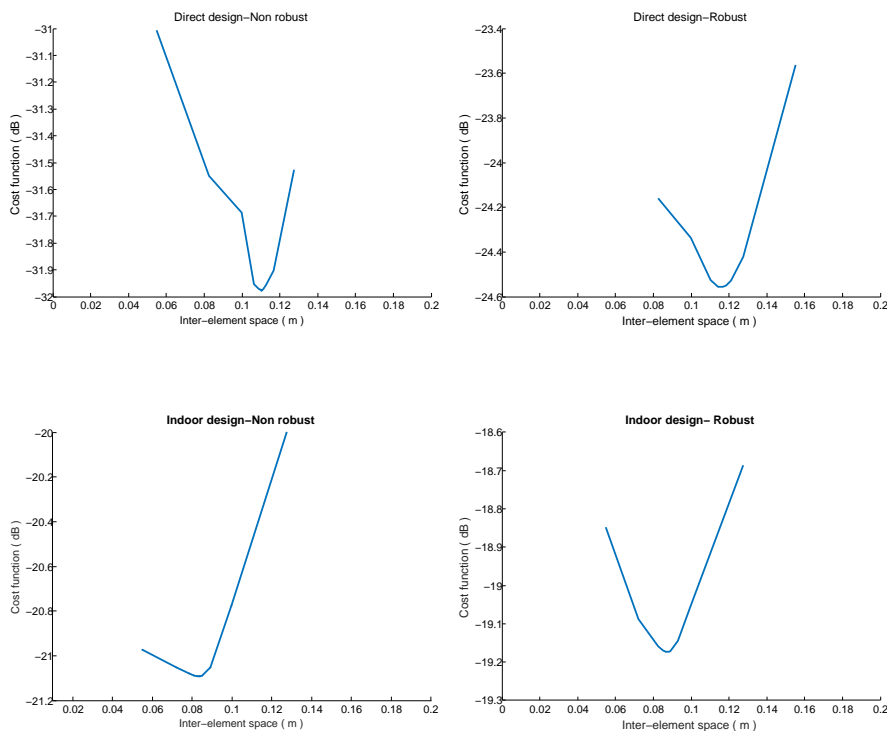
Fig. 9: Cost function comparison for different inter-element spacing among different beamformer designs.

## 9 Acknowledgement

## References

1. Abhayapala, T.D., Kennedy, R.A., Williamson, R.C., Ward, D.B.: Nearfield broadband adaptive beamforming. In: Proceedings of the Fifth International Symposium on Signal Processing and Its Applications, 1999., vol. 2, pp. 839–842. IEEE (1999)
2. Allen, J.B., Berkley, D.A.: Image method for efficiently simulating small-room acoustics. The Journal of the Acoustical Society of America **65**(4), 943–950 (1979)
3. Cauchi, B., Kodrasi, I., Rehr, R., Gerlach, S., Jukić, A., Gerkmann, T., Doclo, S., Goetze, S.: Combination of mvdr beamforming and single-channel spectral processing for enhancing noisy and reverberant speech. EURASIP Journal on Advances in Signal Processing **2015**(1), 61 (2015)
4. Chen, H., Ser, W., Yu, Z.L.: Optimal design of nearfield wideband beamformers robust against errors in microphone array characteristics. Circuits and Systems I: Regular Papers, IEEE Transactions on **54**(9), 1950–1959 (2007)

5. Dam, H.H., Nordholm, S.: Design of robust broadband beamformers with discrete coefficients and least squared criterion. IEEE Trans. Circuits and Systems II: Express Briefs, **60**(12), 897–901 (2013)
6. Doclo, S.: Multi-microphone noise reduction and dereverberation techniques for speech applications (2003)
7. Doclo, S., Kellermann, W., Makino, S., Nordholm, S.E.: Multichannel signal enhancement algorithms for assisted listening devices: Exploiting spatial diversity using multiple microphones. IEEE Signal Processing Magazine **32**(2), 18–30 (2015)
8. Doclo, S., Moonen, M.: Design of broadband beamformers robust against gain and phase errors in the microphone array characteristics. Signal Processing, IEEE Transactions on **51**(10), 2511–2526 (2003)
9. Feng, Z.G., Yiu, K.F.C., Nordholm, S.: Placement design of microphone arrays in near-field broadband beamformers. Signal Processing, IEEE Transactions on **60**(3), 1195–1204 (2012)
10. Frost, O.L.: An algorithm for linearly constrained adaptive array processing. Proceedings of the IEEE **60**(8), 926–935 (1972)
11. Habets, E.A., Benesty, J.: A two-stage beamforming approach for noise reduction and dereverberation. IEEE Transactions on Audio, Speech, and Language Processing **21**(5), 945–958 (2013)
12. Hadad, E., Heese, F., Vary, P., Gannot, S.: Multichannel audio database in various acoustic environments. In: Acoustic Signal Enhancement (IWAENC), 2014 14th International Workshop on, pp. 313–317. IEEE (2014)
13. Khalid, L., Nordholm, S., Dam, H.: Design study on microphone arrays. In: Digital Signal Processing (DSP), 2015 IEEE International Conference on, pp. 1171–1175. IEEE (2015)
14. Kuttruff, H.: Room acoustics. CRC Press (2009)
15. Lehmann, E.A., Johansson, A.M.: Prediction of energy decay in room impulse responses simulated with an image-source model. The Journal of the Acoustical Society of America **124**(1), 269–277 (2008)
16. Li, Z., Yiu, K.F.C., Nordholm, S.E.: On the indoor beamformer design with reverberation. Audio, Speech, and Language Processing, IEEE/ACM Transactions on **22**(8), 1225–1235 (2014)
17. McCowan, I.A., Marro, C., Mauuary, L.: Robust speech recognition using near-field superdirective beamforming with post-filtering. In: icassp, pp. 1723–1726. IEEE (2000)
18. Nahma, L., Dam, H.H.D., Nordholm, S.: Robust beamformer design against mismatch in microphone characteristics and acoustic environments (2018)
19. Naylor, P.A., Gaubitch, N.D.: Speech dereverberation. Springer Science & Business Media (2010)
20. Naylor, P.A., Gaubitch, N.D., Habets, E.A.: Signal-based performance evaluation of dereverberation algorithms. Journal of Electrical and Computer Engineering **2010**, 1 (2010)
21. Nordebo, S., Claesson, I., Nordholm, S.: Adaptive beamforming: spatial filter designed blocking matrix. IEEE Journal of Oceanic Engineering **19**(4), 583–590 (1994)
22. Nordholm, S., Dam, H., Lai, C., Lehmann, E.: Broadband beamforming and optimization. In Zoubir,A.M. (ed), Academic Press Library in Signal Processing:Array and Statistical Signal Processing Massachusetts:Elsevier **3**, 553–598 (2014)
23. Nordholm, S., Rehbock, V., Tee, K., Nordebo, S.: Chebyshev optimization for the design of broadband beamformers in the near field. Circuits and Systems II: Analog and Digital Signal Processing, IEEE Transactions on **45**(1), 141–143 (1998)
24. Rimantho, D., Dam, H.H.H., Nordholm, S.: Design of low complexity robust broadband beamformers with least squared performance criterion (2012)
25. Ryan, J.G., Goubran, R.A.: Array optimization applied in the near field of a microphone array. Speech and Audio Processing, IEEE Transactions on **8**(2), 173–176 (2000)
26. Van Veen, B.D., Buckley, K.M.: Beamforming: A versatile approach to spatial filtering. IEEE assp magazine **5**(2), 4–24 (1988)
27. Yang, B.: Different sensor placement strategies for tdoa based localization. In: Acoustics, Speech and Signal Processing, 2007. ICASSP 2007. IEEE International Conference on, vol. 2, pp. II–1093. IEEE (2007)

28. Yiu, K.F.C., Yang, X., Nordholm, S., Teo, K.L.: Near-field broadband beamformer design via multidimensional semi-infinite-linear programming techniques. Speech and Audio Processing, IEEE Transactions on **11**(6), 725–732 (2003)
29. Zee, M.S., Park, H.M.: Speech dereverberation based on blind estimation of a reverberation filter. IEICE Electronics Express **6**(20), 1456–1461 (2009)
30. Zhao, Y., Liu, W.: Robust fixed frequency invariant beamformer design subject to norm-bounded errors. IEEE Signal Processing Letters **20**(2), 169–172 (2013)
31. Zhao, Y., Liu, W., Langley, R.: Application of the least squares approach to fixed beamformer design with frequency-invariant constraints. IET signal processing **5**(3), 281–291 (2011)
32. Zheng, Y.R., Goubran, R.A., El-Tanany, M.: Robust near-field adaptive beamforming with distance discrimination. IEEE Transactions on speech and audio processing **12**(5), 478–488 (2004)

| Microphone array system parameters | Value |
|---|---|
| Number of elements, M | 9 |
| Interelement spacing | 0.05 m |
| Position of elements | (1.95,3.95,1) , ( 2,3.95,1) , (2.05,3.95,1) , (1.95,4,1) ,(2,4,1) ,(2.05,4,1),(1.95,4.05,1),(2,4.05,1),(2.05,4.05,1) |
| Sampling frequency, $f_s$ | 8 kHz |
| FIR filter length, $L$ | 21taps |
| Weighting functions $V_1$ and $V_2$ | 1 |

Table 6:  Parameters for the evaluation of the microphone array.